Journal of
Materials Chemistry C

Accepted Manuscript

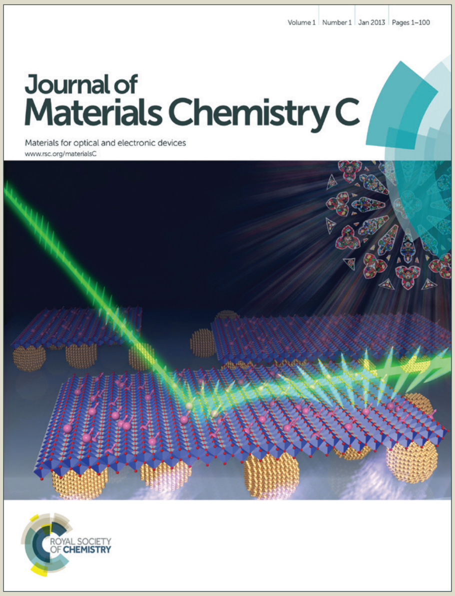

ROYAL SOCIETY
OF CHEMISTRY

www.rsc.org/materialsC

Graphoepitaxial Effect in the Guided Growth of SWNT Arrays on Quartz

Pan Li, Xiao Zhang, Jinghua Li, and Jie Liu*

Department of Chemistry, Duke University, Durham, North Carolina 27708, United States

Abstract

Researchers have demonstrated that the alignment of single-walled carbon nanotubes (SWNTs) on the surface of the single crystal substrate is due to guided growth along either step edges (graphoepitaxial) or certain directions in the atomic lattice (epitaxial), with only one of the two alignment modes predominates in different research system. For the SWNTs grown on quartz surface, the growth of perfectly aligned array and other shapes were induced by the epitaxial effect. Here we report the finding that water vapor introduced during catalyst annealing process can change the alignment mode of the SWNTs on the quartz surface by modifying the surface status of both the catalyst and the substrate. Zigzag shaped nanotube arrays can be obtained by enabling both alignment modes simultaneously through adjusting water vapor concentration, changing the oxidation state of the metal catalyst and/or modifying the morphology of the substrate surface. These findings provide important insights into mechanism of guided growth of complex nanotube shapes, for potential applications including electronics, photodetection, sensing, and other devices.

Introduction

The combination of attractive charge transport and mechanical properties[1, 2] in SWNTs make them excellent candidates for electronic applications, such as flexible electronics,[3] high-speed and power-efficient logic electronics.[4] Large scale of horizontally aligned SWNT arrays and other unique complex geometries are all considered as attractive building blocks.[5-7] Besides expanding the conventional application of SWNTs in flexible devices, bent part of the SWNTs were also found to allow for the electric spin control and coupling and thus benefit applications in spin-based electronics and quantum computation.[8, 9] Researchers have shown that bends can be used to provide electrical control of confined spins, while spins confined in straight segments remain insensitive to electric fields.[10] However, controlled and reproducible placement and alignment of complex SWNT geometries on the substrates remain fundamental issues that need to be solved for real implement of SWNTs in practical devices.

Several strategies have been reported to organize SWNTs into various well-defined geometries. Post-synthetic organizing strategies usually implement liquid flow alignment, which produce SWNT arrays composed of short tubes with limited perfection of alignment.[3, 11-13] Furthermore, complex nanotube geometries, such as rings and loops, have been formed by using affinity templates and microfluidics.[14, 15] Although each of these methods has potential, they still need improvement to offer the levels of perfection useful in electronics. In contrast, chemical vapor deposition (CVD) growth of SWNT array and other complex geometries on crystalline and non-crystalline substrate can produce pristine, long and low-defect nanotubes.[16-20] The most promising approach is considered to be the guided growth on surface of single crystal substrates, where the nanotubes can be aligned by atomic steps or lattice directions. The best growth results of aligned SWNT arrays have been reported on quartz, with perfectly controlled levels of alignment, linearity, average lengths of hundreds of micrometers, and densities as high as 100 SWNTs/μm.[17, 21] Surface-directed growth have yielded many well defined horizontal configurations of SWNTs, such as kinked and wavy nanotubes templated by kinked atomic steps, sawtooth nanofacets and artificial step structures, nanotube serpentines grown by combining surface- and flow-directed growth, and SWNTs adapting the shape of “multiple section stick”.[20, 22-26]

These facts validate the important role played by the surface structure in guiding the alignment of the nanotubes. In all the cases, nanotubes grew either along the atomic lattice or the surface steps.[22, 27-29] Nanotubes formed the minimum-energy configuration by replicating the shape of the underlying surface features due to either epitaxial or graphoeptixial effect. However, density of the nanotubes was relatively low, and properties such as frequency and amplitude of each curved/bent unit was difficult to control. Improvement of the selectivity of specific configuration and the linearity of the straight part is strongly needed to benefit the following device fabrication. Therefore, it is essential to clearly understand the working mechanism of each aligning mode, and further explore the possibility of combing different modes to controllably synthesize complex configurations of SWNTs.

Here we present a method to selectively synthesize a uniquely complex geometry of SWNTs, which bend at multiple points with regular angles. These nanotube structures have been frequently observed but not produced in high yield previously. We also proposed a mechanism of water vapor induced self-organization, in which epitaxial and graphoepitaxial effects compete with each other while guiding the growth of the zigzag shaped SWNTs. Based on the deep understanding of the aligning mechanism, fine control of the morphology of the zigzag nanotubes was realized by adjusting the catalyst composition and the concentration of water vapor in catalyst pretreatment.

Experimental methods

Growth of horizontally aligned SWNT arrays on quartz wafers. Cu catalyst precursor used in the study was a solution of 1.0 mM $CuCl_2$/poly vinylpyrrolidone (PVP) in ethanol. CoMo catalyst precursor solution was prepared by adding molybdenum acetate

$(CH_3COO)_2Mo$ and cobalt acetate hydrate $(CH_3COO)_2Co{\cdot}4H_2O$) into ethanol so that the concentration of Co and Mo over the total solution is 0.02 wt% and 0.08 wt%, respectively. The molar ratio of Co: Mo is 1:3(denoted as Co1Mo3). The mixture was then sonicated for 2 h and diluted by 10 times before use. CoMo catalyst with Co: Mo molar ratio of 1:1 precursor solution (denoted as Co1Mo1) was prepared in the same way by making the concentration of Co and Mo over the total solution as 0.04 wt% and 0.06 wt%, respectively. The catalyst precursor solution were patterned on ST-cut quartz wafers (purchased from http://www.universitywafer.com) following a procedure previously described.[18] The catalyst annealing process included two parts: Firstly the quartz wafers were calcinated at 775°C in air for 15 min to remove polymer and carbon impurities; after the wafers were cooled down to room temperature, the furnace was heated to 775°C, and the wafers dwelt at 775°C for 15 min in H_2 atmosphere. The following CVD growth of SWNTs was carried out at 900°C. A mixed gas of H_2 at ∼180 standard cubic centimeters per minute (sccm), and Ar flow through an ethanol bubbler at ∼80 sccm were introduced into the system. The ethanol bubbler was soaked in the mixture of ice/water and kept at the temperature of 0− 2°C. After 15 min of growth, the Ar gas channel was terminated, and the furnace was cooled down to room temperature while protected by H_2. When needed for annealing, water vapor was produced *in situ* by making tiny controlled H_2 explosion during the calcination at 775^{o}C. The H_2 flow was introduced at ~180 sccm for varied short time, so the amount of water could be adjusted through varying the duration of H_2 introduction. Here 5 s of introduction of H_2 resulted in a water concentration of ~0.3 g/L, 10 s of introduction corresponds to ~0.7 g/L, and 20 s of introduction gives ~1.3 g/L. The detailed calculation about the determination of the exact water concentration was listed in Electronic supplementary information (ESI).

Characterization. A scanning electron microscope (SEM, FEI XL30 S-FEG, operated at 1.5 kV), an atomic force microscope (AFM, Digital Instruments Multi-Mode SPM Nanoscope IIIa, operated in tapping-mode), and a high-resolution transmission electron microscope (HRTEM, Tecnai F20 FEG-TEM, operated at 200 kV) were used to characterize the produced SWNTs. For HRTEM characterization, the samples were transferred from quartz wafers onto the Cu grids covered by holey carbon film (purchased from Electron Microscopy Sciences).

Results and discussion

We first noticed a frequent appearance of zigzag shaped carbon nanotubes (CNTs) when we used Co1Mo3 as catalyst and introduced water vapor during the catalyst annealing, such as those shown in Fig. 1B. Each kinked nanotube consisted of a series of short, straight but misaligned segments, orientated with angles around 42^{o} to the direction of linear tubes. Unlike the growth of perfectly aligned SWNT arrays, production of large amount of the kinked nanotubes could not be satisfactorily explained by the previous guided growth mechanism where only one alignment mode, either atomic steps (graphoepitaxial) or lattice (epitaxial) mode. It is worth noticing that the quartz substrate we used have a miscut angle of 5^o. This induces the spontaneous formation of periodically spaced parallel atomic steps and grooves that have a relative angle of 45^o to the lattice direction. Based on this fact, we hypothesized that the zigzag shaped CNTs could grow under the guidance of two competing forces, which are the epitaxial effect from the lattice and the graphoepitaxial effect from the atomic steps. The formation of these structures could only be driven by interaction between the nanotube and the surface instead of the gas flow, due to the fact that the same set of geometries could always be obtained regardless of the relative position of the lattice to the gas flow. In our hypothesis, the nanotubes first grow along the atomic lattice until they meet steep step or groove, then proceed by following these nanofacets either as single tube or as bundles for a short length, and repeatedly switch between the epitaxial and graphoeptaxial growth modes afterwards. (Fig. 1A).

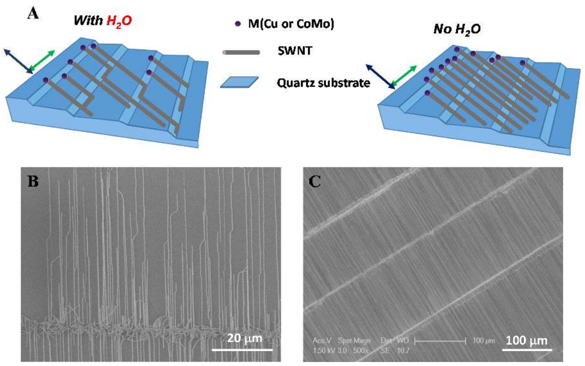

Figure 1. (A)Schematic view of water induced growth of kinked SWNTs (left) versus normal guided growth (right) on miscut ST-cut quartz. Directions of atomic steps and lattice are indicted with green and blue arrows respectively. With either Cu or CoMo as the catalyst, water vapor was discovered to have strong effect on the alignment mode; SEM observation of kinked SWNTs (B) and perfectly aligned SWNTs(C).

To test this hypothesis and the generality of this water-vapor-assisted method, copper-based catalyst, a commonly used catalyst for surface growth of CNTs, was employed to grow CNTs under the same annealing and growth condition. Similar kinked CNT arrays were successfully synthesized with high yield by using the Cu catalyst, as revealed by SEM and AFM, respectively (Fig. 2). A tip-growth mechanism is thus confirmed because a stationary particle cannot push nanotubes forward in such a manner. If the catalyst nanoparticle stays on the substrate without moving together with the tip of the elongating nanotube, the guiding from the substrate will function through interacting with the tip of the nanotube. Thus, for the same tube tip, it is impossible to have different interactions with the crystal lattice and uniformly distributed steps on the substrate. AFM images showed that the perfectly aligned nanotubes grew along the direction of lattice, which is x direction of the ST-cut quartz. Without water vapor treatment, good alignment was obtained even when the atomic steps have height of 1- 3 nm and orientate approximately 42^o to the lattice direction. With water treatment, more kinked nanotubes were observed. Instead of going randomly, the misaligned parts of kinked nanotubes went mostly along the steps.

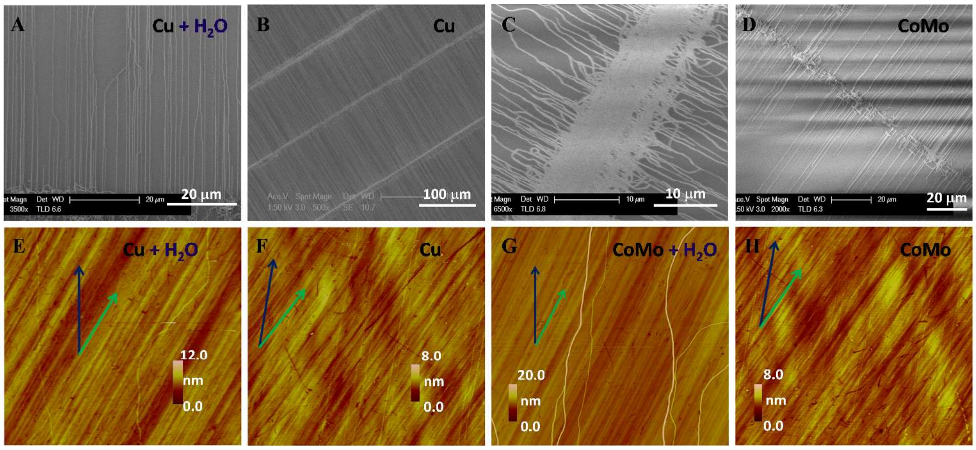

Figure 2. SEM images of SWNTs grown by using Cu-w (A), Cu (B), Co1Mo3-w (C), and Co1Mo3 (D) as catalyst respectively; and corresponding AFM images of SWNTs grown by using Cu-w (E), Cu (F), Co1Mo3-w (G), and Co1Mo3 (H) as catalyst respectively; Green and blue arrows indicate the direction of atomic steps and lattice respectively; The AFM image sizes are 8 × 8 um. The dark stripes in (D) were caused by the charging effect under the e-beam of SEM. Water vapor concentration used for all experiments were 0.7 g/L.

As has been mentioned, treatment with water vapor is key to the growth of kinked nanotubes. For convenience, the catalyst that has been treated with water vapor is denoted as Co1Mo3-w or Cu-w, respectively. Kinked nanotubes grown by Cu-w had both aligned and bent parts with better linearity than that of the Co1Mo3 grown nanotubes, as exemplified in Fig. 2. Cu-w grown kinked nanotubes made turns at angles within a narrow range of ~37^o to ~49^o, centering at 42^o, which is exactly the angle between the steps and lattice direction of the substrate. By contrast, Co1Mo3-w produced kinked nanotubes with almost every part curly using the same concentration of water vapor, while Co1Mo3 could yield well aligned nanotube arrays with high degree of linearity.

One of the primary conclusions could be obtained by analyzing the AFM height images is that, turning character of the nanotubes correlated with its diameter. The small-diameter nanotubes had better alignment, longer part of the tube perfectly aligned along the lattice, and most of the bent part going exactly along the steps. Meanwhile, nanotubes with larger diameters made turns more sharply, and had longer misaligned parts. The largest measured diameter of the nanotube was more than 10.0 nm, which makes this kind of nanotubes probably be bundles instead of single nanotubes. This prediction is later confirmed by HRTEM characterization of the kinked nanotubes. The exact relation between the alignment and the nanotube diameter for different catalyst and annealing conditions were summarized in Fig. 3. For nanotubes grown by Co1Mo3-w catalyst, bending is more likely to happen when the tubes have diameters larger than 1.4 nm. Cu-w catalyzed system has the same trend and almost the same threshold diameter. Besides, bending tubes were rarely observed outside the catalyst pattern area in both Cu and Co1Mo3 catalyzed system. For Cu catalyst, the nanotubes only start to bend when their diameters exceed 3.2 nm, which is considered as bundles. However, in the case of Co1Mo3, all of the nanotubes with diameter bigger than 1.3 nm bent.

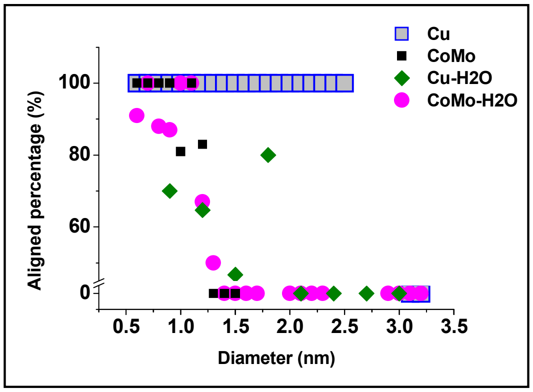

Figure 3. Comparison of templated growth behavior of SWNTs catalyzed by Co1Mo3 and Cu catalyst annealed with/ without water treatment. Plots of the percentage of SWNTs aligned along the lattice direction as a function of SWNT diameter. SWNT diameters were generated from 8 × 8 µm AFM scans of >200 individual SWNTs.

Knowing the composition of the samples, which is the amount of the SWNT, double-walled carbon nanotubes (DWNT) and few-walled carbon nanotubes (FWNT), and bundle of nanotubes, is important to the understanding of the bending mechanism. HRTEM was used to give precise information on the composition of the samples, because AFM cannot distinguish between bundle and a single tube especially when the diameter is not quite large. We used a modified transfer technique (descripted in ESI) to transfer the CNTs from quartz substrate onto the TEM grid. In normal transfer, evaporation of the solvent disturbs the layout of the nanotubes because of the capillary effect when the tubes are not in tight contact with the substrate. Therefore, baking at high temperature, instead of solvent based dissolving, was used to remove the mediate polymer. This approach made the nanotubes maintain their original configuration even over the holey carbon film on the TEM grid. HRTEM characterization showed that 100% of the nanotubes were single-walled, of diameters ranging from 0.8 to 2.2 nm, with no DWNTs or FWNTs found.

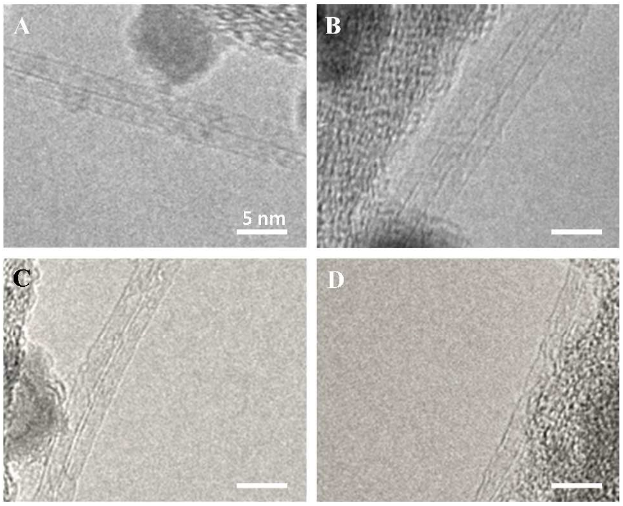

Figure 4. Typical HRTEM characterization result of Co1Mo3-w grown SWNTs (A- B) and Cu grown SWNTs (C-D). Both system yielded high-quality SWNTs with clean surface. The influence of graphoepitaxial effect on the forming and guided growth of big bundles was verified. Bundles appeared with a very high frequency in Co1Mo3-w grown sample. The forming of bundle is believed to account for the large diameter detected by AFM, such like the big bundle with a diameter of 6 nm shown in (B).

Although quantities of nanotubes found under TEM were limited due to the lower density of the kinked tube sample, we were still able to obtain two facts: One is that catalyst treated with water still grew SWNTs, although the nanotubes did not have as good linearity as the nanotubes grown by normally annealed catalyst; and the other is that water treatment of catalyst produced more bundles, which have diameters as big as 6 nm (Fig. 4B). The presence of SWNTs was also confirmed by the abundance of RBM signal and G-band in Raman spectra (ESI). This observation explains why such large diameter "tube" was observed in the Co1Mo3-w system by AFM. It is speculated that, the big bundles were too large to be aligned by either the steps or the lattice. Their overall rigidity, however, was increased, so they could climb over more steep steps when bent away from the lattice direction. This is in agreement with the finding that the bundles or the tubes with bigger diameter could make turns with bigger turning angle and longer length of misaligned part.

Analysis of the annealing process is going to help with understanding the role played by water vapor treatment. In general, Cu precursor decomposed and formed CuO clusters during calcination, which were reduced to metallic Cu during subsequent reduction step. According to earlier studies, the Co1Mo3 catalyst forms Co-molybdate-like species, which remains this interacting phase even after the reduction, and begins converting to metallic Co and Mo carbide under reaction condition.[30] The annealing was carried out at 775^{o}C, which is a temperature high enough to make water a weak oxidizer.[31] Water vapor treatment was proved to be able to oxidize metal catalyst.[32] Therefore, introduction of water vapor is believed to make more of the metal catalyst oxidized, suggesting that both Cu and Co remains as partially reduced clusters for longer time through the whole growth process. In addition, wettability of the particle is strongly related to its oxidation state. It has been experimentally observed that oxidized metal nanoparticles could spread on the support surface (alumina, silica, carbon), because of increased wetting.[33] Related research on the supported catalytic particles also showed that addition of water vapor accelerated overlapping and eventual coalescence of particles, and the migration of catalytic particles on the substrate surface often occurred along steps and was discontinuous.[33] When these partially oxidized particles act as the tip leading the growth of the nanotubes on the quartz substrate, it is expected that the following nanotubes would bend frequently, grow along the steps and form bundles more easily at or close to the edges. Owing to the more Co-molybdate-type initial state, Co1Mo3-w catalysts produce nanotubes that had more kinks and formed more bundles. Partially reduced state of the catalyst could also be a possible reason for the short length of the nanotubes obtained, because the totally reduced metallic state is desired for more efficient growth of nanotubes.

To verify the assumption above, we used Co1Mo1 catalyst, which has been found to have both metallic Co and Co-molybdate-like species after reduction.[30] Compared with Co1Mo3 catalyst and Cu catalyst, the new Co1Mo1 catalyst has less Co-molybdate-like state. As shown in Fig. 5, Co1Mo1 could grow nanotubes that had similar degree of alignment with nanotubes grown by Cu catalyst under the same condition.

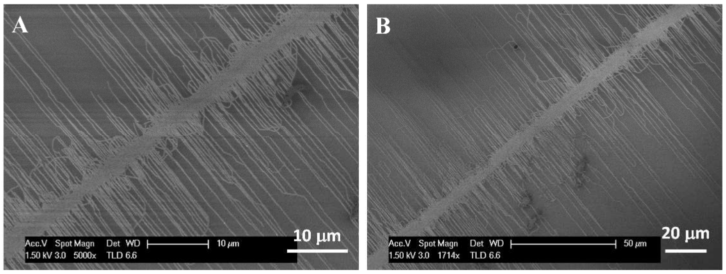

Figure 5. SEM images of SWNTs grown by using Co1Mo1 catalyst with water introduced during annealing. Compared with the nanotubes grown by Co1Mo3 catalyst, the SWNTs shown here have better level of linearity for both aligned and bent parts, as well as lower percentage of the kinked nanotubes.

Different from previous report on the growth of aligned SWNTs,[34] the substrate we used did not undergo annealing process, and the atomic steps formed because of the miscut angle. This 5^{o} miscut angle provides a unique environment to observe the growth of the regularly kinked SWNTs. In order to elucidate how the surface morphology influences the orientation of the nanotubes, we intentionally annealed the quartz substrate to create more atomic steps according to the pervious report.[27] The surface morphology change brought by the annealing was investigated by AFM and shown in ESI. For simplicity of the discussion, we did not introduce water during annealing. As shown in Fig. 6, Cu and Co1Mo3 catalyst could produce well aligned SWNT arrays on both pristine and annealed substrate. However, arrays on the annealed substrate showed shorter tube length and lower density for both kinds of catalysts. These results suggest that too many steps do hinder the movement of the catalyst particles but don't affect the alignment of the nanotubes. This observation also confirmed the tip growth mechanism and the essential role of water on the formation of kinked nanotubes.

Analysis of the impact of water on the morphology of the substrate surface was also done for better understanding. As shown by the section analysis in Fig.S3 and Fig. S4, water treatment made the steps and grooves deeper in both Cu-w and Co1Mo3-w catalyzed system. The deepened steps and grooves produced more kinking on the nanotubes when the catalyst was treated by water.

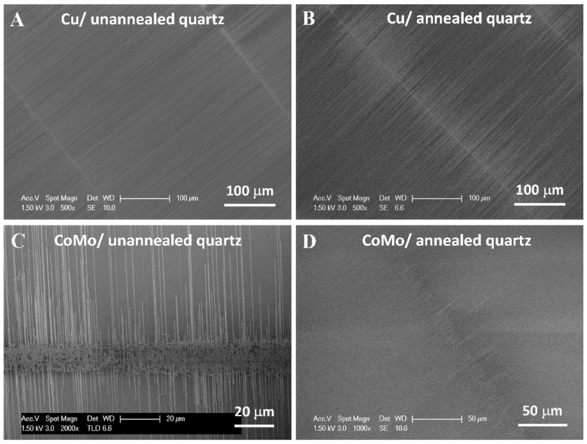

Figure 6. Effect of deepening steps on the guided growth of SWNTs on quartz substrate with different catalyst. SEM images of SWNTs grown by Cu on pristine quartz (A) and on annealed quartz (B); and SEM images of SWNTs grown by Co1Mo3 on pristine quartz (C) and on annealed quartz (D). The substrates were annealed at 900^{o}C for 8h to steepen the steps.

Conclusions

Through controlling the oxidation state of the catalyst, we produced zigzag shaped SWNTs arrays, which is desirable for the fabrication of nanocircuits and the research on the properties of the bending points, on single crystal quartz substrate wit high yield through a combination of epitaxial and graphoepitaxial guiding. The SWNTs were grown following a surface-bound and tip-growth mechanism, and the misalignment is caused by the combination of oxidized state of the metal catalyst and the relatively steep atomic steps and grooves. The introduction of water during annealing alters the oxidation state of the catalyst and enhances the steps and grooves, which cooperatively promote the growth of the zigzag shaped nanotubes. The unique zigzag architecture of nanotube arrays provide an important platform to study the transporting properties of bent nanotubes. In addition, the understanding of alignment mechanism could help the synthesis of novel complex nanotube arrays and benefit the fabrication of nanocircuits.

Electronic supplementary information (ESI) :

Transfer method of SWNTs grown on ST-cut quartz onto SiO_x/Si wafers, water concentration calculation, statistic on the diameter distribution of both aligned and kinked SWNTs in Cu and CoMo catalyzed system, investigation of etching effect of water on quartz substrate under high temperature, Raman characterization of SWNTs, and investigation of influence of annealing on surface morphology of quartz substrate.

Author information

Corresponding Author

*E-mail: j.liu@duke.edu.

Present Address

Department of Chemistry, Duke University, Durham, North Carolina 27708, United States.

Acknowledgements

We are grateful for the support by NSF (CHE-1213469). The authors also acknowledge the support from Duke SMiF (Shared Materials Instrumentation Facilities).

Notes and references

1. R. H. Baughman, A. A. Zakhidov and W. A. de Heer, *Science*, 2002, **297**, 787-792.
2. J. Hu, T. W. Odom and C. M. Lieber, *Accounts of chemical research*, 1999, **32**, 435-445.
3. Q. Cao, H.-s. Kim, N. Pimparkar, J. P. Kulkarni, C. Wang, M. Shim, K. Roy, M. A. Alam and J. A. Rogers, *Nature*, 2008, **454**, 495-500.
4. P. Avouris and R. Martel, *MRS bulletin*, 2010, **35**, 306-313.
5. C. Kocabas, S. Dunham, Q. Cao, K. Cimino, X. Ho, H.-S. Kim, D. Dawson, J. Payne, M. Stuenkel and H. Zhang, *Nano letters*, 2009, **9**, 1937-1943.
6. G. Refael, J. Heo and M. Bockrath, *Physical review letters*, 2007, **98**, 246803.
7. Y. Yao, X. Dai, C. Feng, J. Zhang, X. Liang, L. Ding, W. Choi, J. Y. Choi, J. M. Kim and Z. Liu, *Advanced Materials*, 2009, **21**, 4158-4162.
8. F. Kuemmeth, S. Ilani, D. Ralph and P. McEuen, *Nature*, 2008, **452**, 448-452.
9. T. S. Jespersen, K. Grove-Rasmussen, J. Paaske, K. Muraki, T. Fujisawa, J. Nygard and K. Flensberg, *Nat Phys*, 2011, **7**, 348-353.
10. K. Flensberg and C. M. Marcus, *Physical Review B*, 2010, **81**, 195418.
11. J. Wu, A. Antaris, M. Gong and H. Dai, *Advanced Materials*, 2014, **26**, 6151-6156.
12. Q. Cao, S.-j. Han and G. S. Tulevski, *Nature communications*, 2014, **5**.
13. H. Park, A. Afzali, S.-J. Han, G. S. Tulevski, A. D. Franklin, J. Tersoff, J. B. Hannon and W. Haensch, *Nature nanotechnology*, 2012, **7**, 787-791.
14. Y. Wang, D. Maspoch, S. Zou, G. C. Schatz, R. E. Smalley and C. A. Mirkin, *Proceedings of the National Academy of Sciences of the United States of America*, 2006, **103**, 2026-2031.
15. V. V. Tsukruk, H. Ko and S. Peleshanko, *Physical review letters*, 2004, **92**, 065502.
16. S. J. Kang, C. Kocabas, T. Ozel, M. Shim, N. Pimparkar, M. A. Alam, S. V. Rotkin and J. A. Rogers, *Nature nanotechnology*, 2007, **2**, 230-236.
17. L. Ding, D. Yuan and J. Liu, *Journal of the American Chemical Society*, 2008, **130**, 5428-5429.
18. D. Yuan, L. Ding, H. Chu, Y. Feng, T. P. McNicholas and J. Liu, *Nano letters*, 2008, **8**, 2576-2579.

19. E. Joselevich, *Nano Research*, 2009, **2**, 743-754.
20. N. Geblinger, A. Ismach and E. Joselevich, *Nature nanotechnology*, 2008, **3**, 195-200.
21. C. Kocabas, S. J. Kang, T. Ozel, M. Shim and J. A. Rogers, *The Journal of Physical Chemistry C*, 2007, **111**, 17879-17886.
22. A. Ismach, L. Segev, E. Wachtel and E. Joselevich, *Angewandte Chemie*, 2004, **116**, 6266-6269.
23. A. Ismach, D. Kantorovich and E. Joselevich, *Journal of the American Chemical Society*, 2005, **127**, 11554-11555.
24. N. Shadmi, N. Geblinger, A. Ismach and E. Joselevich, *The Journal of Physical Chemistry C*, 2014, **118**, 14044-14050.
25. Y. Chen, Y. Hu, Y. Fang, P. Li, C. Feng and J. Zhang, *Carbon*, 2012, **50**, 3295-3297.
26. H. Ago, T. Nishi, K. Imamoto, N. Ishigami, M. Tsuji, T. Ikuta and K. Takahashi, *The Journal of Physical Chemistry C*, 2010, **114**, 12925-12930.
27. H. Ago, K. Imamoto, N. Ishigami, R. Ohdo, K.-i. Ikeda and M. Tsuji, *Applied physics letters*, 2007, **90**, 123112-123112-123113.
28. A. Rutkowska, D. Walker, S. Gorfman, P. A. Thomas and J. V. Macpherson, *The Journal of Physical Chemistry C*, 2009, **113**, 17087-17096.
29. J. Xiao, S. Dunham, P. Liu, Y. Zhang, C. Kocabas, L. Moh, Y. Huang, K.-C. Hwang, C. Lu and W. Huang, *Nano letters*, 2009, **9**, 4311-4319.
30. J. E. Herrera, L. Balzano, A. Borgna, W. E. Alvarez and D. E. Resasco, *Journal of Catalysis*, 2001, **204**, 129-145.
31. K. Hata, D. N. Futaba, K. Mizuno, T. Namai, M. Yumura and S. Iijima, *Science*, 2004, **306**, 1362-1364.
32. T. Yamada, A. Maigne, M. Yudasaka, K. Mizuno, D. N. Futaba, M. Yumura, S. Iijima and K. Hata, *Nano Letters*, 2008, **8**, 4288-4292.
33. T. W. Hansen, A. T. DeLaRiva, S. R. Challa and A. K. Datye, *Accounts of chemical research*, 2013, **46**, 1720-1730.
34. S. W. Hong, T. Banks and J. A. Rogers, *Advanced materials*, 2010, **22**, 1826-1830.